

1     **Soil moisture as a potential variable for tracking and quantifying irrigation: a**  
2                     **case study with proximal gamma-ray spectroscopy data**

3     *Paolo Filippucci<sup>1\*</sup>, Angelica Tarpanelli<sup>1</sup>, Christian Massari<sup>1</sup>, Andrea Serafini<sup>2,3</sup>, Virginia Strati<sup>2,3</sup>,*  
4     *Matteo Alberi<sup>2,4</sup>, Kassandra Giulia Cristina Raptis<sup>2,4</sup>, Fabio Mantovani<sup>2,3</sup>, Luca Brocca<sup>1</sup>*

5     <sup>1</sup>Research Institute for Geo-Hydrological Protection, National Research Council, Perugia, Italy

6     <sup>2</sup>Department of Physics and Earth Sciences, University of Ferrara, Via Saragat 1, 44121, Ferrara,  
7     Italy

8     <sup>3</sup>National Institute for Nuclear Physics, Ferrara Section, Via Saragat 1, 44121, Ferrara, Italy

9     <sup>4</sup>National Institute for Nuclear Physics, Legnaro National Laboratories, Viale dell'Università 2,  
10    35020, Legnaro, Italy

11

12

13

14

15

16

17

**June 2018**

18

To be submitted to: *Advances in Water Resources*

19

Declaration of Interest: none

## 20 **Abstract**

21 The global warming effects put in danger global water availability and make necessary to  
22 decrease water wastage, e.g., by monitoring global irrigation. Despite this, global irrigation  
23 information is scarce due to the absence of a solid estimation technique. In this study, we applied an  
24 innovative approach to retrieve irrigation water from high spatial and temporal resolution Soil  
25 Moisture (SM) data obtained from an advanced sensor based on Proximal Gamma-Ray (PGR)  
26 spectroscopy, in a field located in Emilia Romagna (Italy).

27 The results show that SM is a key variable to obtain information about the amount of water  
28 applied to plants, with Pearson correlation between observed and estimated daily irrigation data  
29 ranges from 0.88 to 0.91 by using different calibration methodology. With the aim of reproducing  
30 the working conditions of satellites measuring soil moisture, we sub-sampled SM hourly time series  
31 at larger time steps. The results demonstrated that the methodology is still capable to perform the  
32 daily (weekly) irrigation estimation with Pearson Correlation around 0.6 (0.7) if the time step is not  
33 greater than 36 (48) hours.

34 **Keywords:** SM2RAIN, Irrigation, Soil moisture, Proximal Gamma-Ray method

## 35 **1 Introduction**

36 Irrigation is one of the greatest human intervention on water cycle and it accounts for more  
37 than 70% of global freshwater withdrawals (FAO, 2006; Foley et al., 2011). Nowadays, around  
38 20% of the world's cultivated area is irrigated and it supplies over 40% of the world's food  
39 (Droogers et al., 2010). Global warming and the intensification of the hydrological cycle, with the  
40 increased occurrence of droughts and floods, will threaten the natural availability of water,  
41 enhancing the need of irrigation (Allan & Soden, 2008; Kummu et al., 2016; Rockström et al.,  
42 2012; Vörösmarty et al., 2000). The projected population growth will aggravate this already  
43 complicated panorama, due to the consequent increase of food demand. The knowledge of irrigated  
44 lands and the water used is hence of primary importance to prevent water wastage, to avoid illegal  
45 withdrawals and to ensure food and water security (Siebert et al., 2010; Taylor et al., 2013).  
46 Monitoring irrigation is also fundamental for other applications: (i) to understand the consequences  
47 of irrigation water cycle modifications, (ii) to investigate the impact of irrigation on local and  
48 regional climate conditions, and (iii) to develop hydrological and climate models that account for  
49 irrigation (Sacks et al., 2009).

50 Despite its importance, a global dataset of irrigation water use over long periods is still  
51 missing. Available time series of irrigation amount are mostly based on statistical surveys. This  
52 kind of information does not take into account the illegal pumping and is potentially affected by

53 large errors, because of self-reporting bias, spatial inconsistency and low temporal resolution and  
54 coverage (e.g. the U.S. Geological Survey publishes a report on water use every 5 years) (Deines et  
55 al., 2017). Their quality is hence variable over different states and regions as inferred by Siebert et  
56 al. (2005) who developed a global dataset of area equipped for irrigation by combining sub-  
57 national irrigation statistics. A different approach consists in modelling water requirements for  
58 crop irrigation rather than actual water used for irrigation (Doll & Siebert, 2002; Wada et al., 2014),  
59 but the existence of vast under and over irrigated areas with respect to water requirements (Foley et  
60 al., 2011) represents a large source of errors for this methodology that limits its applicability.

61 In this context, a new source of irrigation information is emerging, i.e. the use of soil  
62 moisture, SM, observations. For decades, SM has been widely used by farmers to efficiently  
63 schedule irrigation (Campbell & Campbell, 1982; Khan et al., 1996; Aguilar et al., 2015). Its  
64 knowledge helps to determine the crop stress conditions and then assists the farmer to decide when  
65 and how much water must be applied for improving the efficiency and the quality of the production.

66 Recently, SM has been also employed to directly quantify the amount of water used for  
67 irrigation (Brocca et al., 2018; Li et al., 2018; Zaussinger et al., 2019). For instance, Li et al. (2018)  
68 used in situ SM data to estimate soil water budget components, including irrigation. The results  
69 show that SM potentially can identify irrigation amounts and frequencies. Zaussinger et al. (2019)  
70 and Brocca et al. (2018) used remote sensing derived SM data. Zaussinger et al. (2019) developed a  
71 methodology to estimate irrigation water use by comparing satellite and modelled SM (which does  
72 not include irrigation information), over the Contiguous United States. They validated the estimated  
73 irrigation amount against the 2013 Farm and Ranch Irrigation Survey (USDA, 2014). Despite the  
74 good results obtained, the validation of the estimated irrigation in different terrains and different  
75 climate conditions appears difficult due to the different period of time of the benchmark dataset  
76 (they considered the 2013 growing season against the satellite data from 2013 to 2017) and its state-  
77 level aggregation.

78 A different approach to estimate irrigation amount from SM has been developed by Brocca et  
79 al. (2018). Through a modified version of SM2RAIN algorithm (Brocca et al., 2014), they  
80 demonstrated that two consecutive satellite soil moisture measurements (in addition to ancillary  
81 rainfall data) can be used to obtain irrigation estimates at daily time scale. The algorithm is based on  
82 an inversion of soil water balance equation to derive the total amount of water entering into the soil.  
83 In practice, from SM measurements the irrigation estimation is possible by subtracting the measured  
84 rainfall fraction from the total water estimated by the algorithm (which inherently includes  
85 irrigation). In Brocca et al. (2018) a preliminary synthetic study, to demonstrate the feasibility of the

86 approach, and a subsequent investigation in nine pilot sites over the world has been performed. Due  
87 to the lack of in situ irrigation data, only qualitative assessment was carried out showing relatively  
88 good agreement of irrigation estimates by different satellite SM products over regions characterized  
89 by long dry periods and in which satellite soil moisture products perform reasonably well. The  
90 method has also been tested by using satellite SM data in two sites, respectively in Nebraska and  
91 Iran (Brocca et al., 2017; Jalilvand et al., 2019), where irrigation data were available.

92 The work of Brocca et al. (2018) and Zaussinger et al. (2019) highlighted some important  
93 limitations mainly related to low spatial and temporal resolution of current available satellite soil  
94 moisture observations. Indeed, most of them have a spatial resolution larger than 20 km, while an  
95 irrigated field can range from few thousands of meters to few squared kilometers. As a result, the  
96 irrigation signal is usually masked out from the presence of other features contained in the coarse  
97 scale satellite pixel. Moreover, a low irrigation signal has a high risk of being indistinguishable  
98 from the inherent noise in the satellite derived SM signal (Su et al., 2015; Massari et al., 2017b).  
99 The use of higher spatial resolution SM observations as those derived from Synthetic Aperture  
100 Radar instruments like Sentinel-1 (Bauer-Marschallinger et al., 2018) could solve this problem for  
101 fields with an area similar to the one of the satellite's pixel (in this case 1 km), but their limited  
102 temporal resolution (one observation every 1.5-4 days over Europe when the two Sentinel-1  
103 satellites are considered) could be inappropriate to detect irrigation applications occurring in few  
104 hours.

105 In summary, three main issues have limited an objective understanding of whether satellite  
106 SM measurements can provide useful information on irrigation estimation, namely, the coarse  
107 spatial support of satellite SM observations, their relatively low temporal resolution (with respect to  
108 the scales of the irrigation practices) and the absence of a reliable benchmark for testing the validity  
109 of the approaches developed so far to estimate irrigation volumes from space.

110 The purpose of this study is to demonstrate that SM is a valuable source of information for  
111 assessing irrigation fluxes and to clarify the effects of spatial and temporal resolution on such  
112 estimates. Specifically, this manuscript aims to answer the following two questions:

- 113 1) is SM a reliable source for retrieving irrigation fluxes?
- 114 2) can the proposed approach be used with high spatial and low temporal resolution  
115 remote sensing data? Can its accuracy be considered sufficient for estimating irrigation?

116 To reach the objectives, we applied the method of Brocca et al. (2018) in a controlled  
117 irrigated experimental field by using an innovative SM dataset inferred from proximal gamma-ray  
118 spectroscopy measurements, characterized by high accuracy, competitive footprint and higher

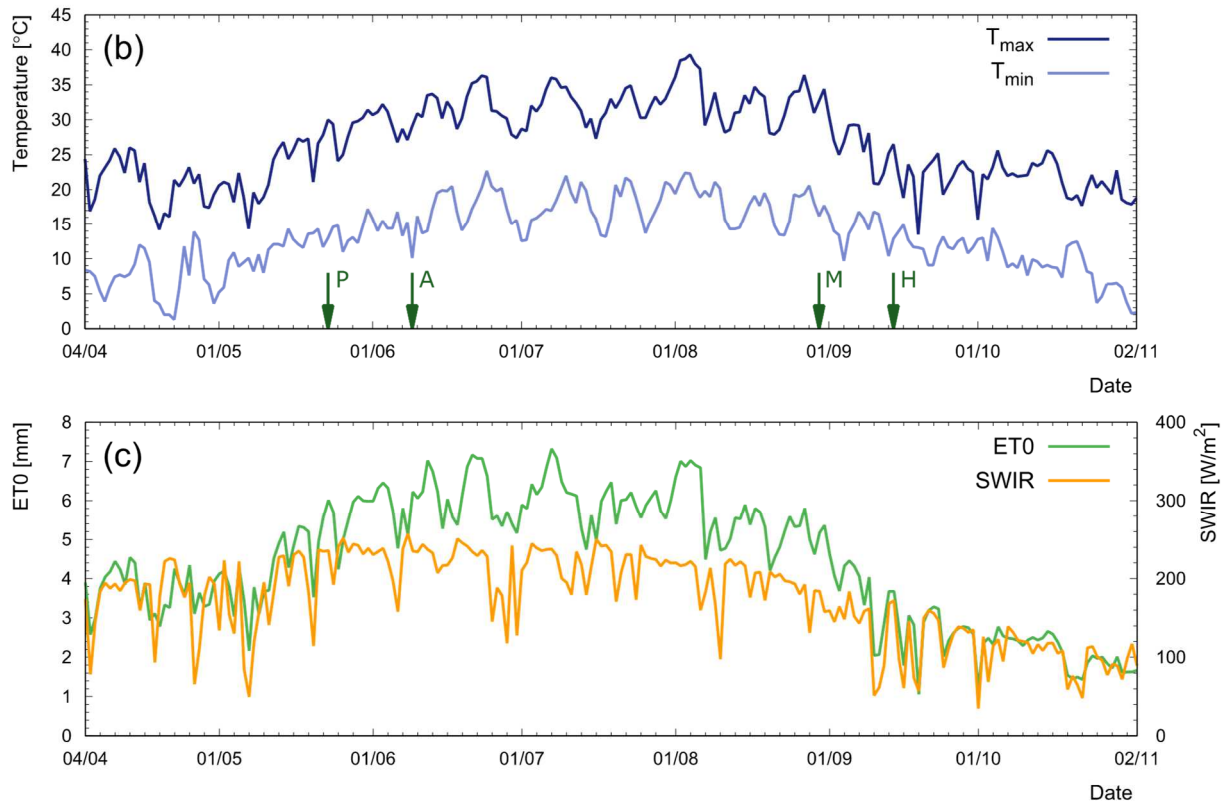
119 temporal resolution with respect to satellite SM data (De Groot et al., 2009; Bogen et al., 2015;  
120 Strati et al., 2018; Baldoncini et al., 2018; Baldoncini et al., 2019). A Proximal Gamma-Ray (PGR)  
121 and an agro-meteorological station have been installed in an experimental field located in North  
122 Italy for a seven-month period. The  $^{40}\text{K}$  gamma signal detected by the PGR spectrometer installed  
123 at a few meters above the ground is inversely correlated with soil water content and it is not affected  
124 by variations in cosmic radiation and soil chemical composition (Strati et al., 2018). The station is  
125 able to sense SM at field scale (Baldoncini et al., 2018), from  $\sim 10^3$  to  $\sim 10^4$  m<sup>2</sup>, and it is therefore  
126 in between point and satellite measurements ( $\sim 10^8$  m<sup>2</sup>), optimal for agricultural application. It is  
127 also characterized by high temporal resolution (1 hour) hence it is able to track SM variations  
128 induced by irrigation.

129 The paper is organized as follows: section 2 presents the description of the experimental site  
130 and setup; section 3 synthesizes how SM can be inferred from PGR spectroscopy measurements and  
131 the basic principles of the proposed algorithm for irrigation estimation; the results, the discussion  
132 and the test at lower temporal resolution are illustrated in section 4. Lastly, conclusions are drawn in  
133 section 5.

## 134 **2 Experimental site and setup**

135 The experimental site is a  $40 \times 108$  m<sup>2</sup> tomato test field ( $44.57^\circ$  N,  $11.53^\circ$  E; 16 m above sea  
136 level) belonging to a research center of the Emiliano-Romagnolo Canal (CER) irrigation district in  
137 the Emilia Romagna region, Italy (Figure 1a). According to the Köppen-Geiger climate  
138 classification (Peel et al., 2007), this geographical area is classified as Cfa (temperate climate,  
139 without dry season and with hot summer). Emilia Romagna is the Italian region having the largest  
140 land surface cultivated with tomatoes, one of the most water-demanding crops among vegetables,  
141 and it contributes for about one third of the tomato national production (ISTAT, 2017).

142 The experimental setup is composed of a Proximal Gamma-Ray, PGR, station equipped with  
143 a 1L NaI(Tl) detector placed at 2.25 m above the ground and a commercial agro-meteorological  
144 station (MeteoSense 2.0, Netsens; see Figure 1a) (Strati et al., 2018). During the data taking period  
145 (from 4 April to 2 November, 2017), the minimum temperature,  $T_{min}$ , ranged from  $1.3^\circ\text{C}$  to  $22.7^\circ\text{C}$   
146 and the maximum temperature,  $T_{max}$ , ranged from 13.5 to 39.3 (Figure 1b); the Short Wave  
147 Incoming Radiation (*SWIR*) varied from 34.7 to 257.3 W/m<sup>2</sup> (Figure 1c). The evapotranspiration  
148 (*ETO*, Figure 1c) is calculated on the basis of the Hargreaves method (Hargreaves & Samani, 1985)  
149 by using weather data recorded by the agro-meteorological station.



150  
 151 *Figure 1. Panel (a), Proximal Gamma-Ray (PGR) and agro-meteorological (AM) stations, and location of the study*  
 152 *area. Panels (b) and (c), weather parameters recorded by the AM station during the data period, i.e. 4<sup>th</sup> of April – 2<sup>nd</sup> of*  
 153 *November 2017: maximum ( $T_{max}$ ) and minimum ( $T_{min}$ ) temperature (panel b), Short Wave Incoming Radiation (SWIR)*  
 154 *and reference evapotranspiration ( $ET_0$ ) (panel c);  $ET_0$  is calculated by using the Hargreaves equation (Hargreaves &*  
 155 *Samani, 1985). The arrows in panel (b) indicate the four major crop maturity phases, i.e., planting (P, 23 May),*  
 156 *anthesis (A, 9 June), maturity (M, 30 August), and harvesting (H, 14 September).*

157 Tomato plants were transplanted on 23 May with a plant density of 3.5 plants/m<sup>2</sup> and  
 158 harvested on 14 September. The crop phenological growth stages of anthesis (the time of flowering)  
 159 and maturity, together with the dates of planting and harvesting, are indicated in Figure 1b.  
 160 Irrigation water was delivered by a sprinkler system, according to a schedule provided by the  
 161 IRRINET decision support tool (Munaretto & Battilani, 2014). The irrigation measurements refer to  
 162 the water pumped to the sprinkler system. In order to account the losses due to leakage, wind drift,

163 spray droplet evaporation and evaporation from leaf surfaces, a scaling factor of 0.9 is applied to  
164 each measurement, as indicated from the field managers.

165 The soil has a loamy texture characterized by 45% of sand, 40% of silt and 15% of clay; soil  
166 bulk density is 1345 kg/m<sup>3</sup> and the organic matter content is 1.26%. The hydraulic properties in  
167 terms of wilting point (0.09 m<sup>3</sup>/m<sup>3</sup>), field capacity (0.32 m<sup>3</sup>/m<sup>3</sup>), and saturation (0.48 m<sup>3</sup>/m<sup>3</sup>) were  
168 inferred from the water retention curve reported in Strati et al. (2018).

## 169 **3 Methods**

### 170 **3.1 Field scale soil moisture monitoring with Gamma-Ray spectroscopy**

171 Nuclear non-invasive and non-contact techniques have been developed for filling the gap  
172 between punctual (~ m<sup>2</sup>) and satellite coarse resolution scale (~ 10<sup>5</sup> m<sup>2</sup>) SM data. The Cosmic-Ray  
173 Neutron and Proximal Gamma-Ray (PGR) methods demonstrated to effectively probe SM with a  
174 field scale footprint (~ 10<sup>4</sup> m<sup>2</sup>) up to a depth of ~ 30 cm, limiting costs and manpower, and using  
175 real-time and wireless sensors (Andreasen et al., 2017; Baldoncini et al., 2018; Strati et al., 2018;  
176 Zreda et al., 2008). In particular, the PGR method consists in the quantification of SM by measuring  
177 gamma signals emitted in the decay of <sup>40</sup>K naturally present and typically homogeneously  
178 distributed in the agricultural soil.

179 A gamma-ray spectroscopy measurement is extremely sensitive to different soil water  
180 contents as water is much more effective in attenuating gamma rays with respect to minerals  
181 typically present in the soil. Indeed, the measured <sup>40</sup>K gamma signal  $S(t)$  [counts per second] at time  
182  $t$  is inversely proportional to the volumetric soil water content SM [m<sup>3</sup>/m<sup>3</sup>] (Baldoncini et al., 2019;  
183 Strati et al., 2018):

$$184 \quad SM(t) = \left( \frac{A(t)}{S(t)} - 0.903 \right) \rho \quad (1)$$

185 with

$$186 \quad A(t) = S^{Cal} \times \Lambda(t) \times [w^{Cal} + 0.903] \quad (2)$$

187 where  $\Lambda(t)$  is the adimensional time dependent biomass water content correction factor (Baldoncini  
188 et al., 2019) and  $\rho$  is the soil bulk dry density (kg/m<sup>3</sup>).  $S^{Cal}$  is the <sup>40</sup>K gamma signal recorded at  
189 calibration time when the gravimetric soil water content  $w^{Cal}$  [kg/kg] was determined on soil  
190 samples.

191 Indeed, the horizontal and vertical horizons of PGR spectroscopy can be defined according to  
 192 the probability law governing the survival of photons when traversing a material, as in Feng et al.  
 193 (2009). Given a fixed detector at ~2 m height and a typical  $1.3 \cdot 10^3 \text{ kg/m}^3$  soil density, it can be  
 194 estimated that 95% of the unscattered gamma photon flux reaching the spectrometer comes from an  
 195 area with a radius of ~ 25 m (Figure 2) and from a depth of ~ 30 cm (Figure 1 of Baldoncini et al.,  
 196 2018).

### 197 **3.2 Quantifying irrigation by the inversion of the water balance equation**

198 The idea to invert the soil water balance equation was initially developed to retrieve rainfall  
 199 from in situ and satellite SM data (Brocca et al., 2015; 2016; 2017; Ciabatta et al., 2017; Koster et  
 200 al., 2016; Massari et al., 2017). Here a similar approach is applied, following the work done by  
 201 Brocca et al. (2018). Specifically, the soil water balance equation for a layer depth  $Z$  can be  
 202 described by the following equation:

$$203 \quad Z \cdot n \cdot \frac{dSM(t)}{dt} = r(t) + i(t) - g(t) - sr(t) - e(t) \quad (3)$$

204 where  $Z$  [mm] is the soil layer depth,  $n$  [ $\text{m}^3/\text{m}^3$ ] is the soil porosity,  $SM(t)$  [-] is the relative  
 205 saturation of soil,  $t$  [days] is the time,  $r(t)$  [mm/days] is the rainfall rate,  $i(t)$  [mm/days] is the  
 206 irrigation rate,  $g(t)$  [mm/days] is the drainage (deep percolation plus subsurface runoff) rate,  $sr(t)$   
 207 [mm/days] is the surface runoff and  $e(t)$  [mm/days] is the actual evapotranspiration. Drainage can  
 208 be expressed by:

$$209 \quad g(t) = a \cdot SM(t)^b \quad (4)$$

210 where  $a$  [mm/days] and  $b$  [-] are two parameters expressing the nonlinearity between drainage rate  
 211 and SM (Brocca et al., 2014).  $sr(t)$  can be considered negligible, since the irrigation through  
 212 sprinkler system should avoid the formation of surface runoff, if carried out optimally. There is still  
 213 the possibility that very intense or frequent water application (rainfall or irrigation) could saturate  
 214 the soil and could lead to surface runoff. The resulting underestimation is a residual error to be  
 215 accepted, since SM cannot keep trace of the runoff. Finally, actual evapotranspiration is assumed  
 216 linearly related to reference evapotranspiration:

$$217 \quad e(t) = ETO \cdot SM(t) \quad (5)$$

218 Therefore, Eq. (3) can be simplified into:



219 
$$r(t) + i(t) = Z^* \cdot \frac{dSM(t)}{dt} + a \cdot SM(t)^b + ET0 \cdot SM(t) \quad (6)$$

220 where  $Z^*$  is  $Z \times n$ .

221 One of the main issues associated with this approach is that the direct inversion of Eq. (6)  
222 inherently leads to false irrigation estimates if the soil moisture signal is highly noisy. To prevent  
223 this problem, a semi-empirical exponential filter (Wagner et al., 1999) was applied to SM data,  
224 which depends on a single parameter representing the characteristic time scale of SM variation,  $T$ .  
225 Once denoised, the SM signal can be used in Eq. (6) to estimate the sum of irrigation and rainfall  
226 rate.

227 The calibration of the three parameters ( $Z^*$ ,  $a$  and  $b$ ) was carried out by minimizing the Root  
228 Mean Square Error (*RMSE*) between observed and estimated rainfall plus irrigation data. In this  
229 perspective, the limited availability of irrigation observation could pose severe limits on the  
230 application of the method. Two different calibration procedures were therefore used to test the  
231 actual need of irrigation observed data: the first calibration (*Rain+Irr* from here onward) is  
232 performed for the entire period using both rainfall and irrigation data, whereas the second one  
233 (*Rain*) is performed by using only rainfall data. For the latter, assuming that no irrigation is applied  
234 when rainfall occurs, the calibration is performed only on days where  $r(t) \neq 0$ . This is a  
235 fundamental hypothesis, because during days in which both rainfall and irrigation occur, the  
236 algorithm will force the total water infiltrated into the soil at the value of the rainfall only, leading  
237 to an underestimation error. The rationale is that if the two calibration procedures provide similar  
238 results in terms of irrigation estimation, the method can be confidently applied with no restrictions  
239 beside the hypothesis above.

240 Once the parameters' calibration is performed, the irrigation rate can be calculated by simply  
241 subtracting the observed rainfall rate from the outcomes of Eq. (6).

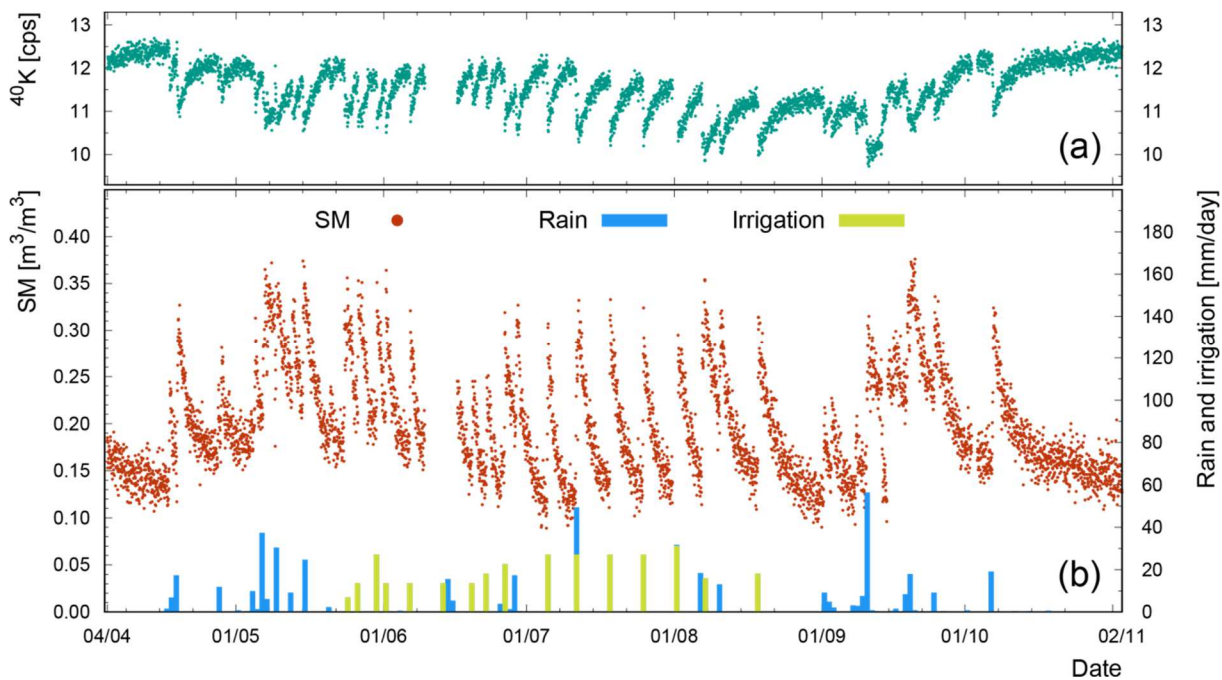
#### 242 **4 Results and discussion**

243 This section describes the estimation of SM from PGR spectra and the estimation of the  
244 irrigation through the application of above presented algorithm. Estimated rainfall and irrigation are  
245 then compared against true rainfall and irrigation fluxes by using two performances indices: the  
246 Pearson Correlation coefficient,  $R$ , and the Root Mean Square Error, *RMSE*. Finally, the role of SM  
247 data temporal resolution is investigated.

248 **4.1 Soil Moisture estimation through Proximal Gamma-Ray spectroscopy**

249 Soil moisture was determined with hourly temporal resolution on the basis of PGR  
250 measurements for almost the entire 7 months data-taking period (Figure 2). The PGR measurement  
251 is sensitive to more than half experimental field and therefore well represents the mean soil  
252 moisture of the field. The gamma and agro-meteorological stations installed at the tomato  
253 experimental field were operative for a 94.8% overlapping duty cycle and a 260 GB global amount  
254 of uncompressed data was recorded. As both stations were equipped with a GPRS connection, it  
255 was possible to remotely process the data in real time.

256 PGR  $^{40}\text{K}$  signal (Figure 2a) and SM (Figure 2b) continuous time series show a strong  
257 correlation with rainfall and/or irrigation events, also in cases of low amounts of distributed water.  
258 PGR measurements are indeed able to provide high frequency SM estimations sensitive to transient  
259 soil water content levels, consistently with physical-hydrological soil properties. The reliability of  
260 the method was tested against validation gravimetric measurements on soil samples, resulting in a  
261  $\sim 2\%$  average discrepancy, and against 3 different soil-crop hydrological models (Strati et al., 2018).

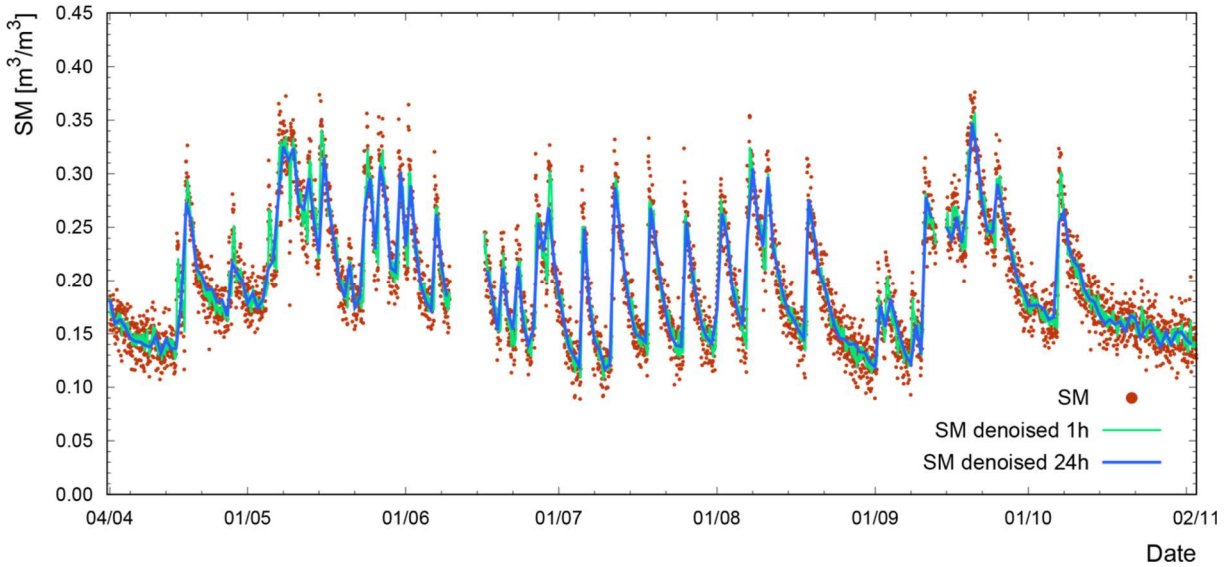


262  
263 *Figure 2. Panel a)  $^{40}\text{K}$  gamma signal in cps (green points), Panel b) volumetric soil water content SM (red points)*  
264 *estimated on the basis of gamma spectroscopy measurements and corrected for the attenuation due to the biomass*  
265 *water content, and daily amount of rainfall (blue lines) and irrigation water (yellow line) are reported for the data*  
266 *taking period (4 April – 2 November).  $^{40}\text{K}$  gamma signals and SM values are hourly averaged.*

267 Provided a calibration of SM through direct measurements on soil samples and a correction  
268 accounting for the biomass shielding effect, PGR spectroscopy performed with a permanent station  
269 can be considered an effective non-stop and non-invasive SM monitoring method.

270 **4.2 From soil moisture to irrigation**

271 PGR SM data were processed through the irrigation estimation algorithm to verify the  
272 feasibility to estimate rainfall and irrigation amounts from SM. An hourly linear interpolation was  
273 applied to estimate SM values during the shutdown periods of the PGR station. If no value was  
274 found within a maximum interpolation gap of 5 hours, the corresponding SM was excluded from  
275 the analysis. The semi-empirical exponential filter was applied to the resulting SM data with 1h  
276 temporal resolution:  $T$  parameter was fixed at 0.16 days (around 4 hours) after the calibration of the  
277 algorithm. The denoised SM data were then sampled every 24 hours at 00:00 UTC to obtain a daily  
278 series of SM used as input of Eq. (6) to predict daily rainfall and irrigation rates. Figure 3 shows the  
279 filtered SM data and the results of the sampling, for the full observation period between April and  
280 November 2017. The data between the 13<sup>th</sup> and the 14<sup>th</sup> of September were masked out due to the  
281 presence of harvesting machines in the field that interfered with the measurements.



282  
283 *Figure 3: Denoised PGR SM time series. The hourly raw data (red circle) are first interpolated with a maximum no*  
284 *data gap of 5h and then filtered with the exponential filter (green line). The resulting data are then sampled each 24h*  
285 *(blue line).*

286 Then, the three parameters of the algorithm ( $Z^*$ ,  $a$  and  $b$ ) were calibrated through an iterative  
287 process, by setting their initial values to the minimum plus 10% of the selected range of variation  
288 (Table 1). The outcomes of the algorithm were finally iteratively compared with the observed  
289 rainfall plus irrigation rates ( $Rain+irr$  calibration) or with the observed rainfall rates ( $Rain$   
290 calibration) until the  $RMSE$  is minimized.

291  
292  
293

	Iteration value		Output calibration value	
	Minimum	Maximum	<i>Rain+Irr</i>	<i>Rain</i>
$Z^*$ [mm]	20.00	200.00	52.08	45.34
$a$ [mm day <sup>-1</sup> ]	0.00	200.00	10.84	12.24
$b$ [-]	1.00	50.00	6.42	3.49

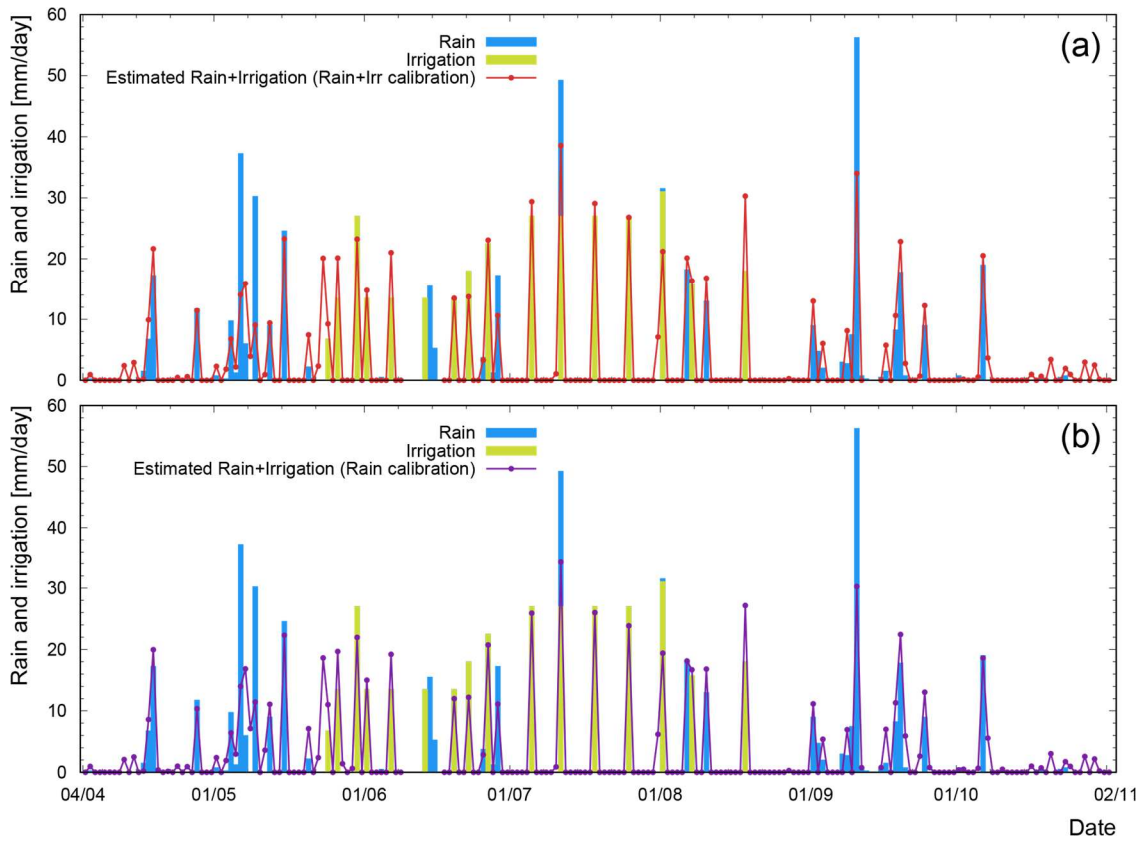
294 Table 1: Calibration parameters ( $Z^*$ ,  $a$  and  $b$ ) of the irrigation estimation algorithm applied to PGR SM data with  
295 rainfall plus irrigation (*Rain+Irr*) and rainfall (*Rain*) calibration. Minimum and maximum iteration values are the  
296 same for both calibration strategies.

297 The optimized values of the parameters are shown in Table 1, for *Rain+Irr* and *Rain*  
298 calibration procedures. The  $Z^*$  parameter value is particularly significant: the PGR station is able to  
299 sense SM until ~300 mm of soil (Figure 1 of Baldoncini et al., 2018), but the gamma contribution is  
300 not uniform with sensing depth. Around 55% of the contribution is derived from the first 50 mm of  
301 soil, rising to 70-80% for the first 100 cm of soil. Considering this and an average porosity around  
302 0.4-0.5, we expected a value of  $Z^*$  around 50, as it is obtained from the calibration of the algorithm.  
303 The variation observed on the parameter values are ascribed to the different calibration period.  
304 Indeed, *Rain* calibration performs the parameters estimation only in days when rainfall occurs.  
305 Nevertheless, the four parameters maintain the same order of magnitude and the obtained results  
306 present just minor differences. The similarities of the two calibration outcomes are also visible in  
307 Figure 4 and Figure 5, where the rainfall and irrigation time series at daily resolution derived on the  
308 basis of the two calibration procedures are shown.

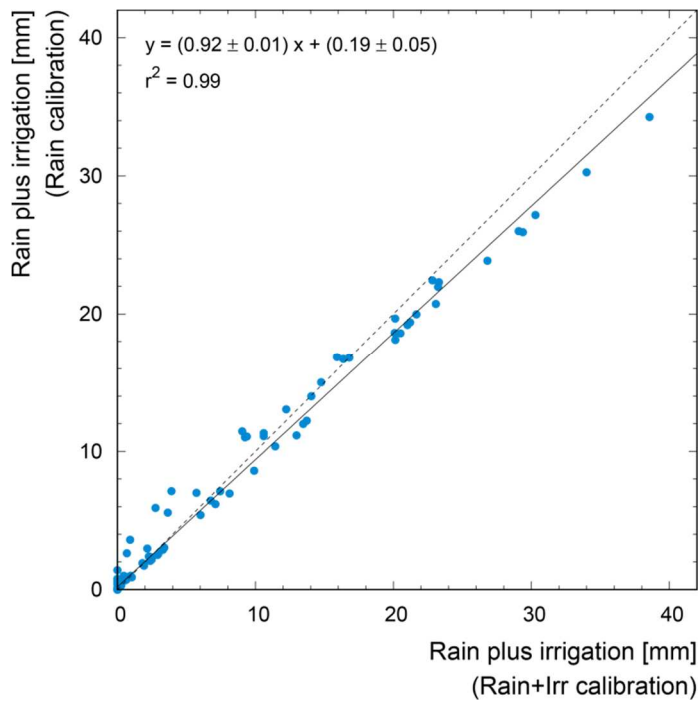
309 Globally, irrigation and rainfall events are successfully detected by the proposed algorithm,  
310 for both calibration procedures. However, the algorithm is not able to well reproduce large  
311 rainfall/irrigation events, particularly if the calibration is carried out with rainfall data only.

312 The irrigation time series are calculated by subtracting the observed rainfall from the  
313 algorithm outcomes. This procedure leads to negative values in correspondence with rainfall  
314 underestimation, e.g. during the months of May and September. Therefore, those values has been  
315 set to zero, since they are not related to the irrigation estimation. For both the calibration  
316 procedures, the total amount of rainfall and irrigation together with the two indices,  $R$  and  $RMSE$   
317 are calculated to evaluate the performance of the proposed algorithm in the estimation of the  
318 irrigation series and the rainfall plus irrigation series with respect to the observed data (see Table 2).

319



320  
 321 *Figure 4. Rainfall plus Irrigation data derived from Rain+Irr calibration (red line, panel a) and Rain calibration*  
 322 *(purple line, panel b) at daily time step. Blue bars represent observed rainfall, yellow bars represent observed*  
 323 *irrigation. .*



324  
 325 *Figure 5. Scatter plot of rainfall plus irrigation data at daily time step obtained after the application of the algorithm*  
 326 *calibrated with Rain+Irr data(x axis ) and with just Rain data(y axis). The black dashed line represents the best fit*  
 327 *linear curve with slope and intercept parameters respectively equal to (0.87±0.01)[mm/mm] and (0.23±0.06) mm and*  
 328 *coefficient of determination  $r^2=0.99$ .*

	<i>Irrigation water</i>			<i>Rainfall plus Irrigation water</i>		
	<i>R [-]</i>	<i>RMSE [mm day<sup>-1</sup>]</i>	<i>Tot [mm]</i>	<i>R [-]</i>	<i>RMSE [mm day<sup>-1</sup>]</i>	<i>Tot [mm]</i>
<i>Rain+Irr calibration</i>	0.90	2.71	460.09	0.89	4.00	742.28
<i>Rain calibration</i>	0.88	2.84	462.45	0.88	4.11	742.65
<i>Observed</i>	/	/	314.55	/	/	752.35

330 Table 2: Comparison between estimated and observed rainfall plus irrigation and just irrigation in terms of Pearson  
331 correlation coefficient, *R*, and Root Mean Square Error, *RMSE*. The total Irrigation and Rainfall plus Irrigation  
332 amounts for observed and estimated series are also shown.

333 The two datasets show very good performances in both the estimation of rainfall plus  
334 irrigation and irrigation with *R* greater than 0.88 in each case. The *RMSE* is around 3 mm/day when  
335 considering just irrigation series and 4 mm/day when considering rainfall plus irrigation series. In  
336 fact, when the irrigation is estimated from rainfall plus irrigation series, negative values are  
337 obtained when rainfall is underestimated. Those values have no physical meanings and are not  
338 related to irrigation, therefore they are set to 0. The error component relative to rainfall  
339 underestimation is hence eliminated and the overall error decreases. This is also demonstrated by  
340 the differences between irrigation and rainfall plus irrigation total error: for each calibration the  
341 irrigation amount is always overestimated, whereas the rainfall plus irrigation amount is  
342 underestimated. The suppression of the negative impact of rainfall underestimation is responsible of  
343 this effect. Finally, the larger underestimation of the outcomes calibrated with just rainfall with  
344 respect to the ones calibrated with both rainfall and irrigation is confirmed by the comparison of the  
345 two calibrations *RMSE* and total water estimated results. As expected, globally *Rain+Irr* calibration  
346 provides better estimates of irrigation with respect to the *Rain* calibration, because even if the  
347 overall overestimation is greater, this is only due to the common rainfall overestimation, i.e. false  
348 irrigation events. The first calibration is better in terms of real estimation of irrigation.

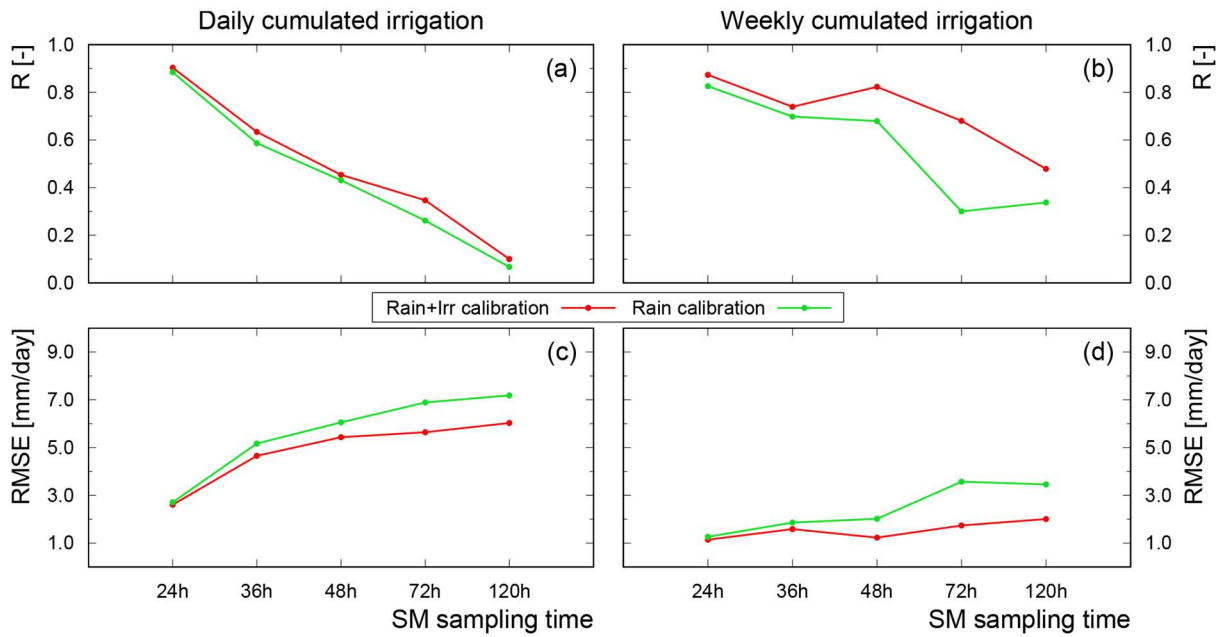
349 Based on the previous analysis, we can answer the first research question. The results show  
350 that PGR SM is indeed a reliable information to perform irrigation estimations. The global lack of  
351 irrigation information for calibration is not a limit for this methodology, as the decrease of  
352 performance when the parameters are calibrated with only rainfall data, is very limited and it can be  
353 imputed to the smaller number of calibration data: i.e. the increase of *RMSE* in estimating rainfall  
354 plus irrigation (irrigation) by using *Rain* calibration rather than *Rain+Irr* calibration is around  
355 2.75% (4.8%) while the decrease in Pearson correlation is around 0.01 (0.02). Hence, the  
356 applicability of this methodology is constrained by the quality of the SM dataset and its spatial and  
357 temporal resolution.

### 358 4.3 Testing satellite temporal resolution

359 The application of the proposed algorithm to PGR SM data demonstrated the potential of  
360 using SM to derive irrigation. The good results obtained support the use of SM with high spatial  
361 resolution. In view of the increased spatial resolution of recent satellite missions for remote SM  
362 sensing, it is necessary to test the effect of a lower temporal resolution. Specifically, synthetic SM  
363 time series were created by down-sampling PGR SM data at 24, 36, 48, 72 and 120 h in order to  
364 reproduce the lower temporal resolution of different remote sensing SM data (e.g., 36 to 144 h for  
365 SMOS, SMAP and Sentinel-1). Then, in order to apply the algorithm for irrigation estimation, the  
366 series were linearly interpolated at daily scale to obtain daily time series of SM from which daily  
367 rainfall and irrigation are computed. As in the previous analysis, the observed rainfall was then  
368 subtracted from the algorithm outcomes to obtain irrigation.

369 A further analysis was carried out by considering the rainfall plus irrigation time series  
370 aggregated at 168h (one week) to average the results in a longer period, (i.e., less affected by the  
371 interpolation approximations). Indeed, the estimation of irrigation at weekly time scale is still useful  
372 for agricultural water management. The performances indices of irrigation series for daily and  
373 weekly analysis are shown in Figure 6.

374 As expected, the irrigation estimation becomes less accurate as the SM sampling time  
375 increases. Nevertheless, the performance drop of daily time series, shown in Figures 6a and 6c, is  
376 clearly worse than that obtained with weekly time series (Figures 6b and 6d). At daily time scale,  
377 the interpolated values deviate from the observed values, but this effect can be averaged by  
378 analyzing a longer period. Still the tendency of decreasing performance remains, probably due to  
379 aliasing problem generated from the sampling procedure, i.e. the missing of some event due to  
380 excessive time step. Figure 6b, in fact, shows that the performance of the weekly product decreases  
381 when SM sampling times greater than 48h are considered. Moreover, the performance for *Rain*  
382 calibration is always lower than that for *Rain+irr* calibration and the discrepancies generally  
383 increase with decreasing temporal resolution. The hypothesis in the *Rain* calibration procedure of  
384 absence of irrigation when rainfall occurs is probably the main responsible of this behavior.



385  
 386 *Figure 6. Comparison between observed and estimated irrigation series derived from SM data at 24, 36, 48, 72 and*  
 387 *120h temporal resolution, cumulated at 24h, (a, c) and 168h (b, d) in terms of Pearson correlation coefficient, R (a, b)*  
 388 *and Root Mean Square Error, RMSE (c, d). Red and green lines correspond respectively to the results obtained with*  
 389 *Rainfall and Irrigation (Rain+Irr) and rainfall (Rain) calibration.*

390 Based on the previous results, we can answer to the second research question. A temporal  
 391 resolution lower than one day can be an issue for daily irrigation estimation. Still the outcomes can  
 392 be acceptable if the temporal resolution is not much greater than 24h (a Pearson correlation  
 393 coefficient of around 0.6 was obtained for the products derived from 36h sampled SM) or if the  
 394 objective is moved from the estimation of daily to weekly irrigation series. In the latter case, we  
 395 obtained good results ( $R > 0.7$ ) for SM time sampling up to 48h. A larger SM sampling time is  
 396 probably too large to correctly follow the natural variation of SM and the performance indices get  
 397 worse.

## 398 5 Conclusions

399 In this study SM data inferred from PGR spectroscopy measurements were used as input for a  
 400 water balance algorithm with the objective to quantify irrigation amount. On the basis of the  
 401 obtained results, the following conclusions can be drawn.

- 402 • PGR spectroscopy proved to be efficient to measure SM at field scale. PGR data with  
 403 hourly frequency are highly sensitive to transient SM levels and are well correlated with  
 404 irrigation and rainfall events. Nevertheless, SM data are quite noisy and needed to be  
 405 filtered.
- 406 • The proposed algorithm to estimate irrigation shows good performances with Pearson  
 407 correlation coefficient between observed and estimated daily irrigation greater than 0.88



408 both when the algorithm is calibrated with daily rainfall and irrigation data and with just  
409 daily rainfall data. In particular, even if the rainfall plus irrigation calibration performs  
410 better, the Pearson correlation between observed and estimated irrigation (rainfall plus  
411 irrigation) decreases by less than 0.02 (0.01) and the RMSE increases by of 4.8% (2.75%)  
412 if the rain calibration is applied, showing that the methodology is applicable also when  
413 irrigation data are absent.

414 • The analysis of data sampled at different time steps, reproducing the lower temporal  
415 resolution of high spatial resolution SM remote sensing data, shows that the methodology  
416 is potentially applicable also in this case if SM sampling times shorter than 48h are  
417 considered. This is the consequence of the drop in performance observed at lower  
418 temporal resolution due to daily interpolation problems and aliasing effect. The impact of  
419 the interpolation can be partially avoided if an aggregation of the results is carried out at  
420 weekly scale.

421 The analysis enabled to address the two research questions above proposed. In particular:

422 1) SM is a reliable source of information for retrieving irrigation amounts and the proposed  
423 algorithm is effective in doing so, even in the case in which only rainfall data are used to  
424 calibrate the algorithm.

425 2) The algorithm performs relatively well with daily data. A lower temporal resolution can  
426 be accepted if the SM sampling time is not greater than 48 h or when the objective is to  
427 obtain irrigation estimates on a time scale longer than one day (e.g. on a weekly time  
428 scale).

429 The main purpose of this study was to assess the capabilities of SM to estimate irrigation water and  
430 the potential application of the proposed methodology to HR remote sensing data. This would  
431 permit to quantify irrigation over large regions (e.g., continental scale) without the need of in situ  
432 stations, while accepting a probable decrease in performance due to the lower spatial and temporal  
433 resolution, and lower accuracy. Further developments in this direction (e.g. the application of the  
434 methodology directly to HR SM remote sensing measurements) are currently being studied and will  
435 be the object of future works

436

437 **Acknowledgments:** We would like to acknowledge the support of European Space Agency  
438 through the project WACMOS-Irrigation (ESA EXPRO RFP/3-14680/16/I-NB).

439 We would like to acknowledge the support of European Space Agency through the project  
440 WACMOS-Irrigation (ESA EXPRO RFP/3-14680/16/I-NB). This research is partially funded by

441 National Institute of Nuclear Physics (INFN) through the ITALian RADioactivity project  
442 (ITALRAD) and by the University of Ferrara (FAR 2019 and Project “Protocolli Operativi Scalabili  
443 per l’agricoltura di precisione - POSITIVE” - CUP: D41F18000080009). The authors thank the  
444 staff of GeoExplorer Impresa Sociale s.r.l. for their support and Stefano Anconelli, Marica  
445 Baldoncini, Marco Bittelli, Carlo Bottardi, Enrico Chiarelli, Giovanni Fiorentini, Domenico  
446 Solimando for enlightening discussions and valuable comments. The authors thank the University  
447 of Ferrara and INFN-Ferrara for the access to the COKA GPU cluster.

- 449 Aguilar, J., Rogers, D., Kisekka, I., 2015. Irrigation Scheduling Based on Soil Moisture Sensors and  
450 Evapotranspiration. Kansas Agricultural Experiment Station Research Reports 1(5)  
451 <http://dx.doi.org/10.4148/2378-5977.1087>.
- 452 Allan, R. P., Soden, B. J., 2008. Atmospheric warming and the amplification of precipitation  
453 extremes. *science* 321(5895), 1481-1484. <http://dx.doi.org/10.1126/science.1160787>
- 454 Andreasen, M., Jensen, K. H., Desilets, D., Franz, T. E., Zreda, M., Bogen, H. R., Looms, M. C.,  
455 2017. Status and perspectives on the cosmic-ray neutron method for soil moisture estimation  
456 and other environmental science applications. *Vadose Zone Journal* 16(8).  
457 <http://dx.doi.org/10.2136/vzj2017.04.0086>
- 458 Baldoncini, M., Albèri, M., Bottardi, C., Chiarelli, E., Raptis, K. G. C., Strati, V., Mantovani, F.,  
459 2018. Investigating the potentialities of Monte Carlo simulation for assessing soil water  
460 content via proximal gamma-ray spectroscopy. *Journal of environmental radioactivity* 192,  
461 105-116. <http://dx.doi.org/10.1016/j.jenvrad.2018.06.001>
- 462 Baldoncini, M., Albèri, M., Bottardi, C., Chiarelli, E., Raptis, K. G. C., Strati, V., Mantovani, F.,  
463 2019. Biomass water content effect in soil water content assessment via proximal gamma-ray  
464 spectroscopy. *Geoderma* 335, 69-77. <http://dx.doi.org/10.1016/j.geoderma.2018.08.012>
- 465 Bauer-Marschallinger, B., Freeman, V., Cao, S., Paulik, C., Schaufler, S., Stachl, T., Modanesi, S.,  
466 Massari, C., Ciabatta, L., Brocca, L., Wagner, W., 2018. Toward Global Soil Moisture  
467 Monitoring With Sentinel-1: Harnessing Assets and Overcoming Obstacles. *IEEE*  
468 *Transactions on Geoscience and Remote Sensing* 99, 1-20.  
469 <http://dx.doi.org/10.1109/TGRS.2018.2858004>
- 470 Bogen, H. R., Huisman, J. A., Güntner, A., Hübner, C., Kusche, J., Jonard, F., Vey, S., Vereecken,  
471 H., 2015. Emerging methods for noninvasive sensing of soil moisture dynamics from field to  
472 catchment scale: A review. *WIREs Water*, 2 (6), 635-647. <https://doi.org/10.1002/wat2.1097>
- 473 Brocca, L., Ciabatta, L., Massari, C., Moramarco, T., Hahn, S., Hasenauer, S., Kidd, R., Dorigo,  
474 W., Wagner, W., Levizzani, V., 2014. Soil as a natural rain gauge: estimating global rainfall  
475 from satellite soil moisture data. *Journal of Geophysical Research: Atmospheres* 119(9),  
476 5128-5141. <http://dx.doi.org/10.1002/2014JD021489>
- 477 Brocca, L., Massari, C., Ciabatta, L., Moramarco, T., Penna, D., Zuecco, G., Pianezzola, L., Borga,  
478 M., Matgen, P., Martínez-Fernández, J., 2015. Rainfall estimation from in situ soil moisture  
479 observations at several sites in Europe: an evaluation of the SM2RAIN algorithm. *Journal of*  
480 *Hydrology and Hydromechanics* 63(3), 201-209. <http://dx.doi.org/10.1515/johh-2015-0016>
- 481 Brocca, L., Pellarin, T., Crow, W. T., Ciabatta, L., Massari, C., Ryu, D., Su, C.-H., Rudiger, C.,  
482 Kerr, Y., 2016. Rainfall estimation by inverting SMOS soil moisture estimates: A comparison  
483 of different methods over Australia. *Journal of Geophysical Research-Atmospheres* 121(20),  
484 12062-12079. <http://dx.doi.org/10.1002/2016JD025382>
- 485 Brocca, L., Ciabatta, L., Massari, C., Camici, S., Tarpanelli, A., 2017. Soil moisture for  
486 hydrological applications: open questions and new opportunities. *Water* 9(2), 140.  
487 <http://dx.doi.org/10.3390/w9020140>
- 488 Brocca, L., Tarpanelli, A., Filippucci, P., Dorigo, W., Zaussinger, F., Gruber, A., Fernandez-Prieto,  
489 D., 2018. How much water is used for irrigation? A new approach exploiting coarse  
490 resolution satellite soil moisture products. *International Journal of Applied Earth Observation*  
491 *and Geoinformation* 73, 752-766. <http://dx.doi.org/10.1016/j.jag.2018.08.023>

- 492 Campbell, G. S., Campbell, M. D., 1982. Irrigation scheduling using soil moisture measurements:  
493 theory and practice. *Advances in irrigation* 1, 25-42. [http://dx.doi.org/10.1016/B978-0-12-](http://dx.doi.org/10.1016/B978-0-12-024301-3.50008-3)  
494 [024301-3.50008-3](http://dx.doi.org/10.1016/B978-0-12-024301-3.50008-3)
- 495 Ciabatta, L., Marra, A. C., Panegrossi, G., Casella, D., Sano, P., Dietrich, S., Massari, C., Brocca,  
496 L., 2017. Daily precipitation estimation through different microwave sensors: Verification  
497 study over Italy. *Journal of Hydrology* 545, 436-450.  
498 <http://dx.doi.org/10.1016/j.jhydrol.2016.12.057>
- 499 De Groot, A. V., Van der Graaf, E. R., De Meijer, R. J., Maučec, M., 2009. Annual Irrigation  
500 Dynamics in the US Northern High Plains Derived from Landsat Satellite Data. *Geophysical*  
501 *Research Letters* 44(18), 9350-9360. <http://dx.doi.org/10.1002/2017GL074071>
- 502 Deines, J. M., Kendall, A. D., Hyndman, D. W., 2017. Annual Irrigation Dynamics in the US  
503 Northern High Plains Derived from Landsat Satellite Data. *Geophysical Research Letters*  
504 44(18), 9350-9360. <http://dx.doi.org/10.1002/2017GL074071>
- 505 Doll, P., Siebert, S., 2002. Global modeling of irrigation water requirements. *Water Resources*  
506 *Research* 38(4), 8-1-8-10. <http://dx.doi.org/10.1029/2001WR000355>
- 507 Droogers, P., Immerzeel, W., Lorite, I., 2010. Estimating actual irrigation application by remotely  
508 sensed evapotranspiration observations. *Agricultural Water Management* 97(9), 1351-1359.  
509 <http://dx.doi.org/10.1016/j.agwat.2010.03.017>
- 510 FAO., 2006. AQUASTAT Online Database. Available at:  
511 <http://www.fao.org/nr/water/aquastat/data/query/index.html>.
- 512 Foley, J. A., Ramankutty, N., Brauman, K. A., Cassidy, E. S., Gerber, J. S., Johnston, M., Mueller,  
513 N. D., O'Connell, C., Ray, D. K., West, P. C., Balzer, C., Bennett, E. M., Carpenter, S. R.,  
514 Hill, J., Monfreda, C., Polasky, S., Rockström, J., Sheehan, J., Siebert, S., Tilman, D., Zaks,  
515 D. P. M., 2011. Solutions for a cultivated planet. *Nature* 478(7369), 337.  
516 <http://dx.doi.org/10.1038/nature10452>
- 517 Hargreaves, G. H., Samani, Z. A., 1985. Reference crop evapotranspiration from temperature.  
518 *Applied engineering in agriculture* 1(2), 96-99. <http://dx.doi.org/10.13031/2013.26773>
- 519 ISTAT, 2017. Estimate of areas and production of agricultural cultivations. Available at:  
520 [http://agri.istat.it/jsp/dawinci.jsp?q=plCPO0000010000023100&an=2017&ig=1&ct=418&id=](http://agri.istat.it/jsp/dawinci.jsp?q=plCPO0000010000023100&an=2017&ig=1&ct=418&id=15A|18A|69A|44A|28A)  
521 [15A|18A|69A|44A|28A](http://agri.istat.it/jsp/dawinci.jsp?q=plCPO0000010000023100&an=2017&ig=1&ct=418&id=15A|18A|69A|44A|28A) (accessed on 20 February 2018).
- 522 Jalilvand, E., Tajrishy, M., Hashemi, S.A.G., Brocca, L., 2019. Quantification of irrigation water  
523 using remote sensing of soil moisture in a semi-arid area. *Remote Sensing of Environment*, in  
524 press. <http://dx.doi.org/10.1016/j.rse.2019.111226>
- 525 Khan, S. R., Rose, R., Haase, D. L., Sabin T. E., 1996. Soil water stress: Its effects on phenology,  
526 physiology, and morphology of containerized Douglas-fir seedlings. *New Forest* 12(1), 19-39.  
527 <https://doi.org/10.1007/BF00029980>
- 528 Koster, R. D., Brocca, L., Crow, W. T., Burgin, M. S., De Lannoy, G. J. M., 2016. Precipitation  
529 estimation using L-band and C-band soil moisture retrievals. *Water Resources Research*  
530 52(9), 7213-7225. <http://dx.doi.org/10.1002/2016WR019024>
- 531 Kummu, M., Guillaume, J., de Moel, H., Eisner, S., Flörke, M., Porkka, M., Siebert, S., Veldkamp,  
532 T. I. E., Ward, P., J., 2016. The world's road to water scarcity: shortage and stress in the 20th  
533 century and pathways towards sustainability. *Scientific reports* 6, 38495.  
534 <http://dx.doi.org/10.1038/srep38495>

- 535 Li, Z., Liu, H., Zhao, W., Yang, Q., Yang, R., Liu, J., 2019. Estimation of Evapotranspiration and  
536 Other Soil Water Budget Components in an Irrigated Agricultural Field of a Desert Oasis,  
537 Using Soil Moisture Measurements. *Hydrology and Earth System Sciences Discussion*.  
538 <https://doi.org/10.5194/hess-2019-89>, in review.
- 539 Massari, C., Crow, W., Brocca, L., 2017. An assessment of the performance of global rainfall  
540 estimates without ground-based observations. *Hydrology and earth system sciences* 21(9),  
541 4347-4361. <http://dx.doi.org/10.5194/hess-21-4347-2017>
- 542 Massari, C., Su, C. H., Brocca, L., Sang, Y. F., Ciabatta, L., Ryu, D., Wagner, W., 2017. Near real  
543 time de-noising of satellite-based soil moisture retrievals: An intercomparison among three  
544 different techniques. *Remote Sensing of Environment* 198, 17-29.  
545 <http://dx.doi.org/10.1016/j.rse.2017.05.037>
- 546 Munaretto, S., Battilani, A., 2014. Irrigation water governance in practice: the case of the Canale  
547 Emiliano Romagnolo district, Italy. *Water Policy* 16(3), 578-594.  
548 <http://dx.doi.org/10.2166/wp.2013.092>
- 549 Peel, M. C., Finlayson, B. L., McMahon, T. A., 2007. Updated world map of the Köppen-Geiger  
550 climate classification. *Hydrology and Earth System Sciences* 11, 1633-1644.  
551 <http://dx.doi.org/10.5194/hess-11-1633-2007>
- 552 Rockström, J., Falkenmark, M., Lannerstad, M., Karlberg, L., 2012. The planetary water drama:  
553 Dual task of feeding humanity and curbing climate change. *Geophysical Research Letters*  
554 39(15). <http://dx.doi.org/10.1029/2012GL051688>
- 555 Sacks, W. J., Cook, B. I., Buening, N., Levis, S., Helkowski, J. H., 2009. Effects of global  
556 irrigation on the near-surface climate. *Climate Dynamics* 33(2-3), 159-175. <http://dx.doi.org/10.1007/s00382-008-0445-z>
- 558 Siebert, S., Burke, J., Faures, J.-M., Frenken, K., Hoogeveen, J., Döll, P., Portmann, F. T., 2010.  
559 Groundwater use for irrigation—a global inventory. *Hydrology and earth system sciences*  
560 14(10), 1863-1880. <http://dx.doi.org/10.5194/hess-14-1863-2010>
- 561 Siebert, S., Döll, P., Hoogeveen, J., Faures, J.-M., Frenken, K., Feick, S., 2005. Development and  
562 validation of the global map of irrigation areas. *Hydrology and Earth System Sciences*  
563 *Discussions* 2(4), 1299-1327. <http://dx.doi.org/10.5194/hess-9-535-2005>
- 564 Strati, V., Albéri, M., Anconelli, S., Baldoncini, M., Bittelli, M., Bottardi, C., Chiarelli, E., Fabbri,  
565 B., Guidi, V., and Raptis, K. G. C., Solimando, D., Tomei, F., Villani, G., Mantovani, F.,  
566 2018. Modelling Soil Water Content in a Tomato Field: Proximal Gamma Ray Spectroscopy  
567 and Soil-Crop System Models. *Agriculture* 8(4), 60.  
568 <http://dx.doi.org/10.3390/agriculture8040060>
- 569 Su, C. H., Narsey, S. Y., Gruber, A., Xaver, A., Chung, D., Ryu, D., Wagner, W. 2015. Evaluation  
570 of post-retrieval de-noising of active and passive microwave satellite soil moisture. *Remote*  
571 *Sensing of Environment* 163, 127-139. <http://dx.doi.org/10.1016/j.rse.2015.03.010>
- 572 Taylor, R. G., Scanlon, B., Döll, P., Rodell, M., Van Beek, R., Wada, Y., Longuevergne, L.,  
573 Leblanc, M., Famiglietti, J. S., Edmunds, M., Konikow, L., Green, T. R., Chen, J., Taniguchi,  
574 M., Bierkens, M. F. P., MacDonald, A., Fan, Y., Maxwell, R. M., Yecheili, Y., Gurdak, J. J.,  
575 Allen, D. M., Shamsudduha, M., Hiscock, K., Yeh, P. J. F., Holman, I., Treidel, H., 2013.  
576 Ground water and climate change. *Nature Climate Change* 3(4), 322.  
577 <http://dx.doi.org/10.1038/nclimate1744>
- 578 USDA., 2014. 2013 Farm and Ranch Irrigation Survey. Available at:  
579 [https://www.nass.usda.gov/Publications/AgCensus/2012/Online\\_Resources/Farm\\_and\\_Ranch](https://www.nass.usda.gov/Publications/AgCensus/2012/Online_Resources/Farm_and_Ranch_Irrigation_Survey/fris13.pdf)  
580 [\\_Irrigation\\_Survey/fris13.pdf](https://www.nass.usda.gov/Publications/AgCensus/2012/Online_Resources/Farm_and_Ranch_Irrigation_Survey/fris13.pdf).

- 581 Vörösmarty, C. J., Green, P., Salisbury, J., Lammers, R. B., 2000. Global water resources:  
582 vulnerability from climate change and population growth. *Science* 289(5477), 284-288.  
583 <http://dx.doi.org/10.1126/science.289.5477.284>
- 584 Wada, Y., Wisser, D., Bierkens, M. F. P., 2014. Global modeling of withdrawal, allocation and  
585 consumptive use of surface water and groundwater resources. *Earth System Dynamics* 5(1),  
586 15-40. <http://dx.doi.org/10.5194/esd-5-15-2014>
- 587 Wagner, W., Lemoine, G., Rott, H., 1999. A method for estimating soil moisture from ERS  
588 scatterometer and soil data. *Remote Sensing of Environment* 70(2), 191-207.  
589 [http://dx.doi.org/10.1016/S0034-4257\(99\)00036-X](http://dx.doi.org/10.1016/S0034-4257(99)00036-X)
- 590 Zaussinger, F., Dorigo, W., Gruber, A., Tarpanelli, A., Filippucci, P., Brocca, L., 2019. Estimating  
591 irrigation water use over the contiguous United States by combining satellite and reanalysis  
592 soil moisture data. *Hydrology and earth system sciences* 23(2), 897-923.  
593 <http://dx.doi.org/10.5194/hess-23-897-2019>
- 594 Zreda, Desilets, D., Ferré, T., Scott, R. L., 2008. Measuring soil moisture content non-invasively at  
595 intermediate spatial scale using cosmic-ray neutrons. *Geophysical Research Letters* 35(21).  
596 <http://dx.doi.org/10.1029/2008GL035655>
- 597